(the 3rd day of this low tide series) quantitative surface samples of tidal water were collected adjacent to an aggregation of *T. gigas* upstream of our research vessel (figure). The tidal flood was dramatically less opaque in comparison to the previous day, due to depletion of zooxanthellae in the reef corals. In spite of this, and the dilution factor caused by mixing of the tidal flood with reef flat waters, millipore (0.22 µm) filtered samples revealed 5.1×10^3 zooxanthellae/l of sea water. Giant clams at this site were actively filter-feeding, as indicated by gaping and inhalant water currents. Examination of the stomach contents from specimens of *T. gigas* feeding upon tidal flood waters in comparison to clams transplanted to a zooxanthellae-free lagoon pool revealed numerous zooxanthellae in the former and their conspicuous absence in the latter. These observations confirm that gastric zooxanthellae are of exogenous origin and not derived from symbionts living in the clams' hypertrophied siphons.

With few exceptions, mass expulsion of zooxanthellae by reef-building corals has gone unrecorded[8,12,13]. Yet at Enewetak Atoll, tidal-cycle data[14] and the reports of local observers suggest that this event occurs frequently, particularly during summer months. The significance of expelled zooxanthellae as a resource for reef organisms is an intriguing question. Traditionally, zooxanthellae have been viewed as 'imprisoned phytoplankton'[15] which are unavailable to reef dwelling filter-feeders. We have discovered that *Tridacna* utilizes exogenous zooxanthellae following their release by heat-stressed hermatypic corals, but it is also likely that modest numbers of suspended zooxanthellae are available to reef organisms on a continuing basis. Recent evidence suggests that coral polyps may control the population size of their intracellular zooxanthellae via the ongoing expulsion of the older and less metabolically active algae[9]. These data, and the distinctive habitat of giant clams, always being located on or near reef-forming corals[7], indicate that exogenous zooxanthellae are an important, perhaps obligatory, constituent of nutriment for *Tridacna.*

1 We are grateful to personnel of the Mid-Pacific Marine Laboratory, Enewetak Atoll, Marshall Islands, and Friday Harbor Laboratories, Washington, for providing services and facilities where portions of this study were performed. Financial support was provided by the US Department of Energy and by operating grants from the National Research Council of Canada. We thank Drs Eugene N. Kozloff and Richard R. Strathmann for comments.

2 T.F. Goreau, N.I. Goreau and C.M. Yonge, J. Zool., Lond. *169,* 417 (1973).
3 C.M. Yonge, Sci. Am. *232,* 96 (1975).
4 B.S. Morton, J. Zool., Lond. *185,* 371 (1978).
5 K. Mansour, Nature *157,* 844 (1946).
6 C.M. Yonge, J. Zool., Lond. *123,* 551 (1953).
7 P.V. Fankboner, Ph.D. Thesis, University of Victoria, B.C., 1972.
8 J. Rosewater, Indo-Pacific Mollusca *1,* 347 (1965).
9 C.M. Yonge and A.G. Nicholls, Scient. Rep. Gt Barrier Reef Exped. *V 1,* 177 (1931).
10 T.F. Goreau, N.I. Goreau and T.J. Goreau, Sci. Am. *241,* 124 (1979).
11 H.T. Odum and E.P. Odum, Ecol. Monogr. *25,* 291 (1955).
12 L. Muscatine, in: Biology and Geology of Coral Reefs, vol. 2. Ed. O.A. Jones and R. Endean. Academic Press, New York 1973.
13 D.F. Squires, Nature *195,* 361 (1962).
14 T.F. Goreau, Science *145,* 383 (1964).
15 Admiralty Tide Tables, Pacific Region. H.M. Stationary Office, London 1979.
16 C.M. Yonge, in: Advances in Marine Biology, vol. 1. Ed. F.S. Russel. Academic Press, New York 1963.

Increasing porosity of the incubating alligator eggshell caused by extrinsic microbial degradation[1]

M. W. J. Ferguson

Anatomy Department, The Queen's University of Belfast, Medical Biology Centre, 97 Lisburn Road, Belfast, BT9 7BL (Northern Ireland), 30 September 1980

Summary. The outer densely calcified layer of the alligator eggshell shows progressive crystal dissolution, with the production of concentrically stepped erosion craters, as incubation progresses. This dissolution is caused by the acidic metabolic byproducts of nest bacteria. Extrinsic degradation serves to gradually increase the porosity and decrease the strength of the eggshell.

The nesting American alligator *(Alligator mississippiensis)* lays eggs in the centre of a mound of vegetation[2,3], and after 65 days of incubation the young hatch[4]. During incubation the eggshell becomes stained due to the ingress of microorganisms[5] (as far as the eggshell membrane), extensive cracks develop throughout its length[4] and eventually it flakes off the eggshell membrane a few days before hatching, so that the young alligator has only to slit the latter with its egg caruncle before emerging from the 'egg'. Alligator farmers have successfully incubated eggs in trays of nesting media (mostly Spartina patens) at nest temperatures (28 °C) and humidities (100%)[6]. However if alligator eggs are incubated without nesting media (as in experimental embryological investigations[5,7-9]), the young develop fairly normally but fail to hatch due to an abnormally tough eggshell. In order to investigate this phenomenon and to determine the percentages of minerals that the alligator fetus removes from the egg during incubation (for 'shell less culture' and eggshell windowing experiments) the structure and composition of the alligator eggshell were investigated in 396 specimens removed from eggs at daily intervals throughout the 65-day incubation period (details of methods used given in Ferguson[5]). The alligator eggshell consists from the surface inwards of an outer densely calcified zone (approx. 100–200 µm thick), a honeycomb zone (approx. 300–400 µm thick) and a mammillary zone (approx. 20–30 µm thick) to which is attached the eggshell membrane (approx. 150–250 µm thick). The entire eggshell is composed of small rhombohedral crystals of calcite (figure 1, A) interspersed with a variable amount of organic matrix. In the outer densely calcified zone there is no detectable organic matrix and the calcite crystals are regularly stacked in vertical layers on their a faces (figures 1, A, C–J; 3 and 4) with their c axes at right angles to a tangent to the shell surface at any point (figures 1, C–J; 3 and 4). Contrariwise in the honeycomb zone there is a higher percentage of organic matrix which creates a meshwork of vesicular holes between the calcite crystals; and these holes

interconnent with the egg contents via spaces between the mammillae and pores in the eggshell membrane. Furthermore, in the honeycomb zone, the calcite crystals are regularly stacked in horizontal layers on their b faces (figures 1, A, C–J) with their a axes at right angles to a tangent to the shell surface at any point.

At the time of egg laying numerous small surface defects (figure 1, C) are present in the outer densely calcified layer, where either crystals have failed to form or have been knocked out as the eggs clink together when they are deposited in the nest one after the other. As incubation progresses these small defects increase in size and depth to produce erosion craters with characteristic stepped concentric rings (figures 2 and 3). Each of these rings is one crystal high (figures 3 and 4) and corresponds to a layer of calcite crystals in the outer densely calcified zone (figures 1, C–J; 3 and 4). Numerous microorganisms are present around the surface defects and erosion craters (figure 2). These microorganisms produce acidic metabolites as a product of fermenting the decaying nest vegetation; and these acids in combination with carbonic acid (generated by the hydration of expired carbon dioxide) dissolve the calcite crystals in the outer densely calcified layers enlarging the surface defects into erosion craters (figures 2 and 3), in much the same way that acidogenic oral bacteria decalcify tooth enamel to produce dental caries[10]. The method of formation of the erosion craters is illustrated diagrammatically in figures 1, C–J. The stepped pattern of concentric rings is

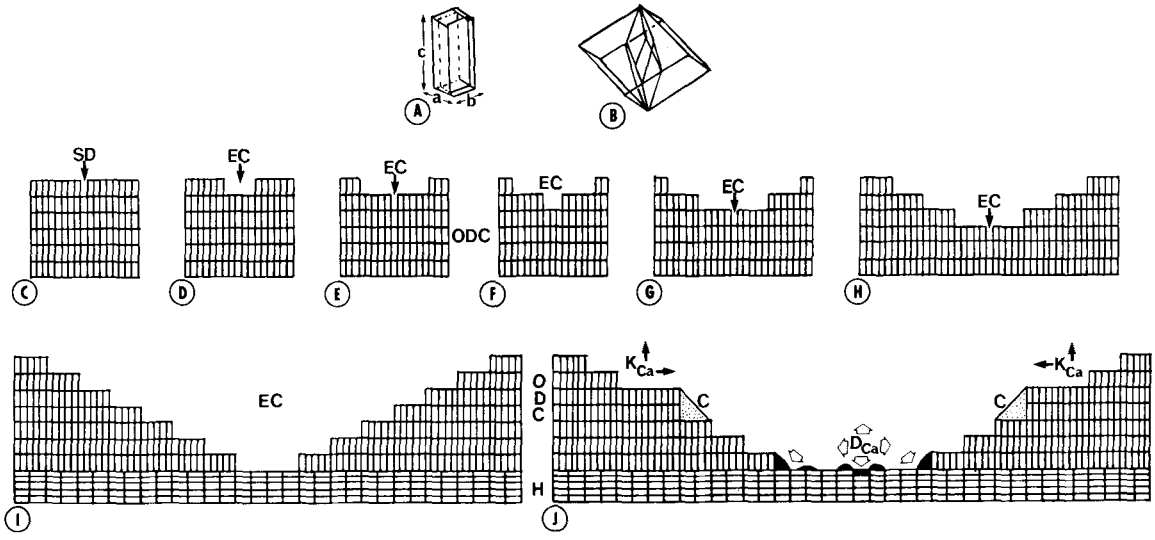

Fig. 1. *A* A habit of calcite $CaCO_3$ Class 3m (after Bunn 1945[11]) illustrating the general shape of the crystal and the direction of its axes a, b and c. *B* A large (32-molecule) unit rhombohedron of calcite based on cleavage rhomb. The true unit cell is the small (2-molecule) steep rhombohedron shown inside (after Bunn 1945[11]). *C–J* Series of diagrams illustrating the formation of erosion craters (EC) in the outer densely calcified layer (ODC) of the shell. SD = surface defect, e.g. a crystal missing, H = honeycomb layer (crystals stacked horizontally as opposed to vertically in the outer densely calcified layer), D_{Ca} and open arrows = diffusion control with dissolution and reprecipitation of calcium (indicated by black areas), K_{Ca} = kinetic control, C = remnants of cuticle or organic debris.

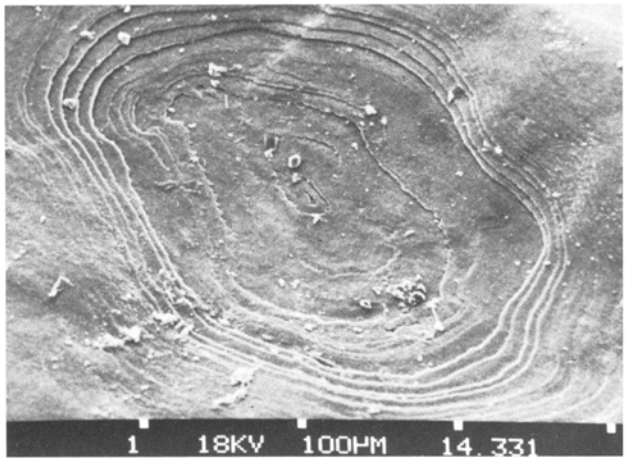

Fig. 2. Scanning electron micrograph of the surface of an alligator egg 43 days after laying. Note the regular concentrically stepped rings of the erosion crater, and the remnants of nesting debris and microorganisms.

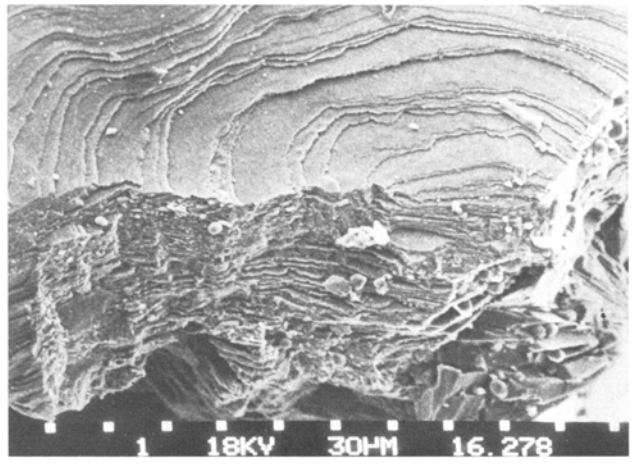

Fig. 3. Scanning electron micrograph of the surface and radially fractured (by natural cracking) edge of an erosion crater in an alligator egg 48 days after laying. Note the numerous layers of vertically stacked calcite crystals in the outer densely calcified zone which correspond with the eroded concentric rings of the erosion crater.

caused by the regular stacking of the calcite crystals (figures 3 and 4) and their anisotropic properties, i.e. the c faces of the crystals dissolve faster than either the a or b faces[11-13] (figure 1, C-J). The dissolution of the outer layers of calcite crystals is largely under kinetic control (figures 1, J; 3 and 5) since the dissolved minerals can diffuse into the adjacent nesting media while the acid is replenished at the shell surface (figure 1, J). However remnants of cuticle or organic debris may mask certain layers of crystals so causing irregularities in the stepped contour (figures 1, J and 2). The erosion craters dissolve through all the layers of the outer densely calcified zone (figures 1, C-J, 2, 3 and 4) and finally develop broad bases on the honeycomb layer,

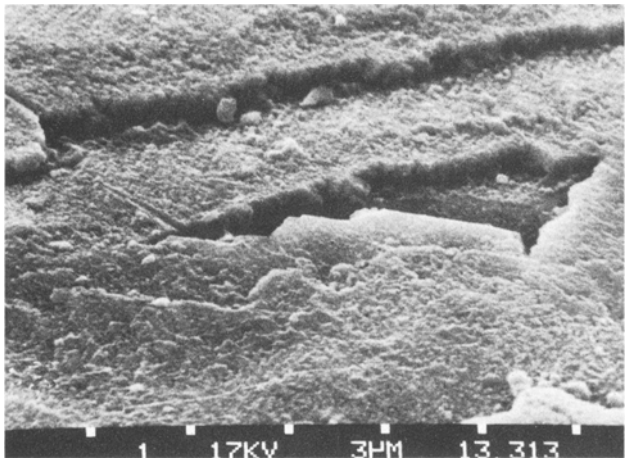

Fig. 4. Higher power scanning electron micrograph of the base of the erosion crater seen in Fig. 2. Note that each of the concentric rings of the crater is 1 calcite crystal high, and that this corresponds with the vertical stacking of single calcite crystals (with their a faces one on top of the other) in the outer densely calcified zone (figure 3).

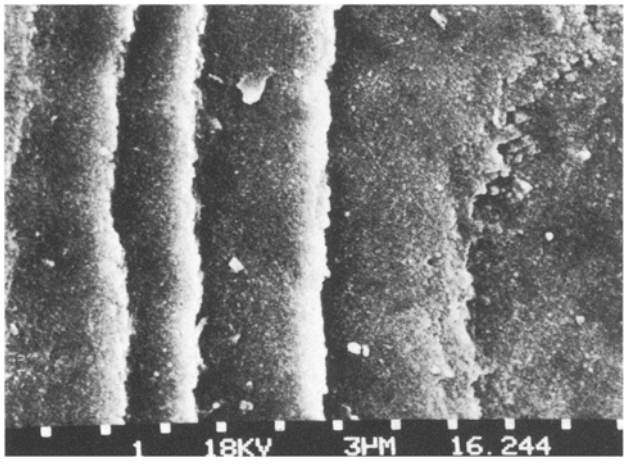

Fig. 5. Higher power scanning electron micrograph of the concentric rings of an erosion crater in a day-48 alligator egg viewed at 90° to the shell surface. To the left of the picture are the sharp symmetrical outer rings of the erosion crater, where the dissolution of the layers of calcite crystals is under kinetic control. To the right of the picture is the basal aspect of the erosion crater where the acidic dissolution of the layers of calcite crystals is under diffusion control: here the erosion ring is neither as clearly defined, nor as symmetrical as in the outer layers and in addition it shows evidence of mineral reprecipitation - compare with figure 1.

where the calcite crystals are orientated with their more resistant (to acid dissolution) b faces uppermost (figures 1, I-J). Furthermore the dissolution of the lower layers of calcite crystals is under diffusion control (figures 1, J, 2 and 5) as manifest by the reprecipitation of dissolved eggshell mnnerals and the loss of the sharp concentrically stepped edges of the erosion craters (figures 1, J and 5). The change in orientation of the calcite crystals from the outer densely calcified zone to the honeycomb zone plus the operation of diffusion control prevent the eggshell from completely dissolving under this extrinsic acidic attack (figure 1, J). The hypothesis that extrinsic acid is responsible for the formation of the erosion craters was tested by dripping carbonic acid (pH = 6) onto the surface of freshly laid, pore and crater free eggshell fragments, for 24 h and then viewing the specimens in the SEM. Concentrically stepped erosion craters identical to those seen in vivo (figure 2) are produced by this treatment. The numerous cracks which develop in the eggshell as incubation progresses always pass through the erosion craters (figure 3). It is postulated that the development of these craters weakens the eggshell and facilitates cracking, in much the same way that it is easier to tear paper along perforations. In addition, the development of the erosion craters exposes large areas of the underlying porous honeycomb zone at the crater base (figures 1, I and J), which doubtlessly assist in the exchange of respiratory gases between the ever enlarging fetus and the external environment. This increasing porosity as incubation proceeds is important as no air space develops in the alligator egg while conventional pores are present only in the centre of the eggshell[5]. The tortous pathway of the fine vesicular holes from the crater base to the egg contents prevent microbial invasion of the latter.

The structure of the alligator eggshell is beautifully adapted to both its function and the nesting biology of the animal. Thus, at the time of laying, the eggs have a high initial strength and are not very porous, which obviously prevents damage to (and dehydration of) the eggs as they are deposited one after the other in the nest and the female treads nest vegetation on top of them. As incubation progresses, extrinsic acidic degradation of the eggshell exposes large areas of the honeycomb zone at the bases of the erosion craters, so making the shell more porous and thereby facilitating the exchange of respiratory gases and water vapour from the ever enlarging alligator fetus. The erosion craters also weaken the eggshell causing it to crack and fall off the eggshell membrane about 60 days, so facilitating hatching at 65 days. This cleavage is assisted by the removal of small calcite crystals from the upper layers of the mammillary zone for use in fetal mineralisation[5]. The alligator fetus obtains approximately. 2.4 times as much calcium from the shell as from the egg contents (most birds obtain about 5 times as much[5,14]). This is the first time that normal extrinsic degradation of the eggshell of any animal has been described and the first report of the ability of an eggshell to change its porosity as incubation progresses. It is unknown if the nest microorganisms derive any benefit (e.g. calcium) from this process. It would be interesting to learn whether the eggs of other crocodilians, which are often laid in a sandy hole as opposed to a nest of vegetation[2,3], also show this extrinsic degradation. It would be equally interesting to investigate whether or not the eggs of other animals, e.g. dinosaurs show signs of extrinsic degradation: this may suggest how such a system evolved phylogenetically. It is very important when alligator eggs are artificially incubated, that they are completely surrounded by nesting media at 28 °C and 100% humidity, otherwise if nesting media is excluded, the young never hatch through the abnormally tough shell and quickly die from asphyxiation.

1 The work is supported by M.R.C. grant No. G979/386/CB and E.H.S.S.B. grant No. EB 109/74/75.
2 A.E. Greer, Nature *227*, 523 (1970).
3 H.W. Campbell, Nature *238*, 404 (1972).
4 T. Joanen, Proc. 23rd A. Conf. Southeastern Association Game and Fish Commissioners, p. 141 (1969).
5 M.W.J. Ferguson, J. Zool., in press (1981).
6 T. Joanen and L. McNease, Int. Zoo Yb. *19*, 61 (1979).
7 M.W.J. Ferguson, Med. Hypoth. *5*, 1079 (1979).
8 M.W.J. Ferguson, J. Anat. *129*, 851 (1979).
9 M.W.J. Ferguson, Arch. oral Biol., in press (1981).
10 G.N. Jenkins, The physiology and biochemistry of the mouth, 4th edn. Blackwell, Oxford 1978.
11 C.W. Bunn, Chemical Crystallography. Clarendon Press, Oxford 1945.
12 A.K. Galwey, Chemistry of Solids. Chapman & Hall, London 1967.
13 P.W. Atkins, Physical Chemistry. Oxford University Press, Oxford 1978.
14 N.K. Jenkins, Comp. Biochem. Phys. *51A*, 891 (1975).

Cell transformation of frozen human fibroblasts by a strong magnetic field? – A reinvestigation

E. Haigis, R. Gitzelmann and H. Ott

Division of Metabolism, Department of Pediatrics, University of Zürich, Kinderspital, CH-8032 Zürich (Switzerland), and Laboratorium für Festkörperphysik, ETH-Hönggerberg, CH-8093 Zürich (Switzerland), 17 September 1980

Summary. A magnetic field of 5000 Gs did not induce morphological transformations of human skin and lung cells in culture as reported previously by Malinin et al.

Recently Malinin et al. reported 'evidence of morphological and physiological transformation of mammalian cells by strong magnetic fields'[1]. They exposed frozen cells at 4.2 °K to a magnetic field of 5000 Gs for 4–8 h. For human lung fibroblasts (WI-38 cells) changes were described as follows: The rate of growth was markedly inhibited; cultures failed to maintain a consistent monolayer; cells piled up; contact inhibition was abolished or markedly altered; morphologically distinct, enormously elongated cells were observed; strongly basophilic nuclei were characterized by coarse chromatin which tended to display intranuclear axial symmetry; nucleoli tended to lose their spherical shape and to be oriented in association with the axially symmetric chromatin network and there was an abundance of giant nuclei with the same characteristics.

We tried to reproduce these phenomena with human lung fibroblasts (WI-38 cells, obtained from Flow Laboratories, Irvine, Scotland), and with human skin fibroblasts established from healthy adults in our laboratory. Cells were cultivated in Falcon plastic flasks (75 cm^2) under standard conditions (37 °C, 95% air, 5% CO_2) in Eagle's minimal essential medium (MEM) to which were added fetal calf serum (GIBCO), glutamine, penicillin, streptomycin, amphotericin-B and sodium bicarbonate to give final concentrations of 10%, 2 mM, 100.000 units/l, 100 mg/l, 0.25 mg/l and 12 mM respectively. The WI-38 cells were in passages 29-31, the human skin fibroblasts in passages 15-16. All cultures were free of mycoplasma as tested by the fluorochrome procedure[2]. Cells from each flask were harvested by trypsinization, suspended in 1.8 ml culture medium supplemented with 0.2 ml of dimethylsulfoxide (DMSO), frozen slowly and stored in 2-ml vials in liquid nitrogen. Vials were inserted into a rack which fitted the cryostat inside the bore of a superconducting magnet and secured immobility of the samples. The vials were transported in liquid nitrogen to the precooled (78 °K) cryostat, immediately mounted into the center of the superconducting solenoid and the compartment was further cooled with liquid helium. The temperature of the cells was never above 80 °K, and they were cooled to liquid helium temperature within approximately 15 min. The temperature was monitored by means of a resistance thermometer mounted on the rack. When the temperature of the rack had reached 4.2 °K the magnetic field was slowly activated to 5000 Gs within approximately 1 min. The cells remained exposed to this stationary magnetic field for 4 h. After removing the magnetic field with about the same sweep rate, the cells were transferred back to the liquid nitrogen container. Control cells were handled identically but the magnetic field was not activated. 8 vials of each cell line were exposed to the magnetic field and 8 vials of each line served as controls.

Treated cells were thawed after storage periods varying from 20 h to 1 week to 4 months and transferred at different concentrations to small petri dishes (Falcon plastics) for culture. Cells of each vial were also grown on glass cover slips in petri dishes. Cultured cells were examined for morphological appearance and growth pattern. Nuclei of cells grown on cover slips were inspected before and after fixation with methanol/glacial acetic acid (3/1; vol/vol) and staining with orcein.

None of the cell lines, neither the WI-38 lung cells nor the human skin fibroblasts, showed any of the changes of growth or form described previously[1]. Sample cells could not be distinguished from control cells nor from cells that had never been exposed to liquid helium. Rate of growth, cell shape and contact inhibition appeared normal. It seems clear that the effects observed by Malinin et al.[1] cannot be ascribed solely to the influence of the strong magnetic field applied[3].

Acknowledgment. Magnet and low temperature equipment were financed in part by the Schweizerischer Nationalfonds zur Förderung der wissenschaftlichen Forschung.

1 G. I. Malinin, W.D. Gregory, L. Morelli, V.K. Sharma and J.C. Houck, Science *194*, 844 (1976).
2 W.C. Russell, C. Newman and D.H. Williamson, Nature *253*, 461 (1975).
3 We assume that the glutamine supplement to MEM was not '2 mmole per ml' as indicated in Malinin et al.[1] but in fact 2 µmole per ml.